DRAFT VERSION MAY 27, 1998
Preprint typeset using LaTeX style emulateapj

THE EFFECT OF AN ISOTHERMAL ATMOSPHERE ON THE PROPAGATION OF THREE-DIMENSIONAL WAVES IN A THERMALLY STRATIFIED ACCRETION DISK

G. I. OGILVIE[1,3] AND S. H. LUBOW[2,3]

Submitted to the Astrophysical Journal

ABSTRACT

We extend our analysis of the three-dimensional response of a vertically polytropic disk to tidal forcing at Lindblad resonances by including the effects of a disk atmosphere. The atmosphere is modeled as an isothermal layer that joins smoothly on to an underlying polytropic layer. The launched wave progressively enters the atmosphere as it propagates away from the resonance. The wave never propagates vertically, however, and the wave energy rises to a (finite) characteristic height in the atmosphere. The increase of wave amplitude associated with this process of wave channeling is reduced by the effect of the atmosphere. For waves of large azimuthal mode number m generated by giant planets embedded in a disk, the increase in wave amplitude is still substantial enough to be likely to dissipate the wave energy by shocks for even modest optical depths ($\tau \gtrsim 10$) over a radial distance of a few times the disk thickness. For low-m waves generated in circumstellar disks in binary stars, the effects of wave channeling are less important and the level of wave nonlinearity increases by less than a factor of 10 in going from the disk edge to the disk center. For circumbinary disks, the effects of wave channeling remain important, even for modest values of optical depth.

Subject headings: accretion, accretion disks — hydrodynamics — waves

1. INTRODUCTION

Tidally generated waves can play an important role in the dynamics of gaseous disks and the tidal perturbers. The Lindblad resonances (LRs) are important sites of wave generation in disks (Goldreich & Tremaine 1979). Most previous studies have approximated the disk as two-dimensional (2D) by ignoring effects in the vertical direction (perpendicular to the orbit plane). For disks whose structure and thermodynamic response are locally vertically isothermal, the 2D approximation accurately describes the wave that is generated at an LR, which is indeed a 2D sound wave. In many cases of astrophysical interest, however, the disk is thermally stratified (optically thick) in the vertical direction. Such cases include the planet-forming regions of protostellar disks (Bell et al. 1997) and cataclysmic variable (CV) disks (La Dous 1994).

In an earlier paper (Lubow & Ogilvie 1998, hereafter Paper I), we analyzed the linear response of a thin, vertically polytropic disk to tidal forcing at LRs. We found that the dominant mode of excitation was the f mode of even symmetry. Close to the resonance, this mode behaves compressibly and occupies the full vertical extent of the disk, like the 2D mode in an isothermal disk. However, as the wave propagates away from the resonance through a radial distance of order r_L/m (for resonance radius r_L and azimuthal mode number m), it behaves incompressibly, like a surface gravity mode, and becomes confined close to the disk surface. The degree of confinement increases with distance from the resonance. As a consequence of this wave-channeling process, there is usually a strong increase in wave amplitude with radial distance from the LR on the scale r_L/m. Although this analysis did not include damping or nonlinear effects explicitly, we estimated that shocks would sometimes develop and damp the wave. Other damping mechanisms such as radiative damping (Cassen & Woolum 1996) or viscous damping may also be of importance.

Once the wave energy is channeled to a region close to the disk surface, the wave's properties are determined by the structure of the disk's outer layers. In particular, the effects of a disk atmosphere can be important. Such effects are not well represented by a vertically polytropic disk. In the case of a polytrope, there is a definite surface on which the density and temperature drop to zero. With an atmosphere, the disk density drops more gradually with height and the temperature is approximately constant. In fact, there is no actual disk surface in the isothermal case. The density falls as a Gaussian with height above the midplane. In the limit of very high (vertical) optical depth in the disk, the polytropic approximation should be adequate because the atmosphere contains an insignificant fraction of the disk's mass. In the opposite limit of an optically thin disk, the disk structure is vertically isothermal and the wave launched at resonance behaves as a 2D sound wave.

The purpose of this paper is to determine to consequences of a finite, non-zero optical depth on the propagation of a wave launched from an LR. For disks of optical depth of about 100, which is thought to be typical in planet-forming regions of protostellar disks, nearly one per cent of the disk's mass resides in the atmosphere. As a result of wave channeling, the wave energy could be contained within the atmosphere. The purpose of this paper is to explore the consequences of a disk atmosphere on the propagational properties of the waves generated at LRs. We aim to determine whether the wave in the disk

[1]Institute of Astronomy, University of Cambridge, Madingley Road, Cambridge CB3 0HA, United Kingdom
[2]Space Telescope Science Institute, 3700 San Martin Drive, Baltimore, MD 21218
[3]Isaac Newton Institute, University of Cambridge, 20 Clarkson Road, Cambridge CB3 0EH, United Kingdom

atmosphere would propagate upwards into very low density regions where shock dissipation would occur. More generally, we want to determine how much the wave amplitudes can be amplified by the wave-channeling process in the presence of a disk atmosphere as a function of disk optical depth.

2. DESCRIPTION OF THE MODEL

The semi-analytic approach taken in Paper I can be extended to include the disk atmosphere, which is modeled as an isothermal layer that extends from some height above the mid-plane outward. Beneath this layer resides a thermally stratified polytropic layer which extends vertically down to the mid-plane. For convenience, we treat the transition as abrupt, although in reality it may occur over a distance comparable to a scale height.

As will be shown, physical solutions to the wave equation in the isothermal layer can be obtained analytically. The upper boundary condition of the isothermal layer is that no waves carry energy from great distances above the disk mid-plane downwards toward the mid-plane. That is, there are no external sources of energy above the disk. The solutions allow for the possibility of reflection in the disk atmosphere and propagation to great (or infinite) heights in the atmosphere.

These atmospheric solutions contain some freedom that needs to be constrained by the underlying polytropic layer. The isothermal solutions provide constraints that serve as an outer boundary condition for the numerical solution of the wave equations in the polytropic layer. Taken together, vertically global solutions are obtained that connect the two layers in a physically meaningful manner. The ratio of the temperature at mid-plane to the temperature at the layer interface determines the disk optical depth through the T–τ relation.

3. EQUILIBRIUM OF THE DISK

The disk is considered to be a steady, axisymmetric fluid rotating in a constant, axisymmetric gravitational potential. Referred to cylindrical polar coordinates (r, ϕ, z), the fluid has angular velocity $\Omega(r,z)$, density $\rho(r,z)$, and pressure $p(r,z)$, while the gravitational potential is $\Phi(r,z)$. The disk is considered to be thin, so that the angular velocity can be considered independent of z and given by

$$r\Omega^2 = \left.\frac{\partial \Phi}{\partial r}\right|_{z=0}, \tag{1}$$

while the epicyclic frequency κ is given by

$$\kappa^2 = 4\Omega^2 + 2r\Omega\frac{\mathrm{d}\Omega}{\mathrm{d}r}. \tag{2}$$

The effective gravitational acceleration is $-g(r,z)\,\mathbf{e}_z$, where

$$g = \Omega_\perp^2 z, \tag{3}$$

and $\Omega_\perp(r)$ is the vertical frequency given by

$$\Omega_\perp^2 = \left.\frac{\partial^2 \Phi}{\partial z^2}\right|_{z=0}. \tag{4}$$

In particular, we will be interested in a Keplerian disk about a spherical mass M, for which the potential is

$$\Phi = -GM(r^2+z^2)^{-1/2} \tag{5}$$

and $\kappa = \Omega_\perp = \Omega$. However, the notational distinction between Ω, κ, and $\Omega_\perp$ is retained, partly to aid the interpretation of the equations in the case of a Keplerian disk, and partly to allow a generalization to non-Keplerian disks.

The local vertical equilibrium of the disk is determined by the equation

$$\frac{\partial p}{\partial z} = -\rho g. \tag{6}$$

The buoyancy frequency $N(r,z)$ of vertical oscillations is given by

$$N^2 = g\left(\frac{1}{\gamma p}\frac{\partial p}{\partial z} - \frac{1}{\rho}\frac{\partial \rho}{\partial z}\right), \tag{7}$$

where γ is the adiabatic exponent. Throughout this paper, the self-gravitation of the fluid, its viscosity, and the accretion flow are neglected.

In order to model a disk of finite optical depth, we assume that the pressure and density are related by a polytropic relation,

$$p = K\rho^{1+1/s}, \tag{8}$$

in a central layer $|z| < z_1$ containing the mid-plane, and by an isothermal relation,

$$p = c^2\rho, \tag{9}$$

in the outer layers $|z| > z_1$. The pressure and density are required to be continuous at the interface. The solution is then

$$|z| < z_1 : \ \rho = \rho_0\left(1 - \frac{z^2}{H_s^2}\right)^s, \tag{10}$$

$$|z| > z_1 : \ \rho = \rho_0\left(1 - \frac{z_1^2}{H_s^2}\right)^s \exp\left[-\frac{(z^2-z_1^2)}{2H^2}\right] \tag{11}$$

for the density, and

$$|z| < z_1 : \ p = p_0\left(1 - \frac{z^2}{H_s^2}\right)^{s+1}, \tag{12}$$

$$|z| > z_1 : \ p = p_0\left(1 - \frac{z_1^2}{H_s^2}\right)^{s+1} \exp\left[-\frac{(z^2-z_1^2)}{2H^2}\right] \tag{13}$$

for the pressure. Here $\rho_0(r)$ and $p_0(r)$ are the density and pressure on the mid-plane, and $H = c/\Omega_\perp$ is the isothermal scale height. The quantity H_s is the height at which the polytropic layer would reach zero density and pressure if it were not truncated, and is given by

$$H_s^2 = \frac{2(s+1)p_0}{\Omega_\perp^2\rho_0}. \tag{14}$$

Furthermore, the relation

$$H_s^2 - z_1^2 = 2(s+1)H^2 \tag{15}$$

holds, because dp/dz is continuous at the interface.

The quantity z_1/H_s is a measure of the 'weighting' assigned to the polytropic layer in this mixed model. The

ratio of the temperature of the isothermal layer to the temperature at the mid-plane (for an ideal gas) is

$$\frac{T_{\rm i}}{T_{\rm m}} = 1 - \frac{z_1^2}{H_g^2}. \tag{16}$$

This may be expressed in terms of an approximate effective optical depth τ at the mid-plane according to the relation (e.g. Bell et al. 1997)

$$T_{\rm m}^4 = \tfrac{3}{8}\tau T_{\rm i}^4, \tag{17}$$

which gives

$$\tau = \tfrac{8}{3}\left(1 - \frac{z_1^2}{H_g^2}\right)^{-4}. \tag{18}$$

The ratio $\Sigma_{\rm i}/\Sigma_{\rm p}$ of the surface densities of the two layers can be expressed in terms of z_1/H_g, but only by using higher transcendental functions.

We assume that the effective adiabatic exponent γ is constant and greater than unity in the central layer, but equal to unity in the outer layers. This reflects the fact that the thermal time-scale is short compared to the dynamical time-scale in the isothermal layers.

The buoyancy frequency may then be evaluated as

$$|z| < z_1 : \; N^2 = \left[s - \left(\frac{s+1}{\gamma}\right)\right]\left(\frac{2z^2}{H_g^2 - z^2}\right)\Omega_\perp^2, \tag{19}$$

$$|z| > z_1 : \; N^2 = 0, \tag{20}$$

and is discontinuous at $|z| = z_1$.

4. DESCRIPTION OF THE LOCAL DISPERSION RELATION

4.1. *Basic equations*

The equations governing free, linear waves in a thin accretion disk have been derived and solved in different cases by Lubow & Pringle (1993, hereafter LP), Korycansky & Pringle (1995), Ogilvie (1998), and in Paper I. The separation of scales between the horizontal and vertical directions allows all wave quantities to be expressed as WKB functions in r, except in the neighborhood of resonances, which are also turning points for the waves. In particular, a wave quantity X assumes the form

$$X(r,\phi,z,t) \sim \mathrm{Re}\left\{\bar{X}(r,z) \times \exp\left[-i\omega t + im\phi + i\int k(r)\,dr\right]\right\}, \tag{21}$$

where ω is the frequency eigenvalue, m is the azimuthal wavenumber and $k(r)$ is the radial wavenumber. The tilde will be omitted hereafter. The equations satisfied by the Eulerian velocity perturbation (u,v,w) and pressure perturbation p' at each radius may be written

$$\rho(\hat{\omega}^2 - \kappa^2)u = \hat{\omega}kp', \tag{22}$$

$$\rho(\hat{\omega}^2 - N^2)w = -i\hat{\omega}\left(\frac{\partial p'}{\partial z} + \frac{gp'}{v_{\rm s}^2}\right), \tag{23}$$

and

$$-i\hat{\omega}p' = -\gamma p\left(iku + \frac{\partial w}{\partial z}\right) + \rho g w, \tag{24}$$

where $v_{\rm s} = (\gamma p/\rho)^{1/2}$ is the sound speed and

$$\hat{\omega} = \omega - m\Omega \tag{25}$$

is the intrinsic frequency of the wave. The azimuthal velocity perturbation is related to the radial one by

$$-i\hat{\omega}v + 2Bu = 0, \tag{26}$$

where

$$B = \Omega + \frac{r}{2}\frac{d\Omega}{dr} \tag{27}$$

is the usual Oort parameter.

4.2. *Analytical solutions in the isothermal layer*

LP solved analytically for the vertical structure of modes in a purely isothermal disk by obtaining series solutions of the equations about $z = 0$. The relevant solutions were identified as terminating power series (i.e. polynomials) of either even or odd symmetry, multiplied by an exponential factor. In the present case, we must consider more general solutions because different boundary conditions apply at the interface between the two layers.

In the isothermal layer, equations (22)–(24) may be rewritten as

$$\frac{\partial u}{\partial z} = \left(\frac{\hat{\omega}^2}{\hat{\omega}^2 - \kappa^2}\right)ikw \tag{28}$$

and

$$\frac{\partial w}{\partial z} = \left(\frac{1}{ik}\right)\left[k^2 - \left(\frac{\hat{\omega}^2 - \kappa^2}{\Omega_\perp^2}\right)\frac{1}{H^2}\right]u + \left(\frac{z}{H^2}\right)w. \tag{29}$$

There exists a 2D mode consisting of a purely horizontal motion independent of z, which satisfies the dispersion relation

$$\hat{\omega}^2 = \kappa^2 + c^2k^2. \tag{30}$$

For all other modes, equations (28) and (29) can be combined to give a single, second-order equation for w in the form

$$\frac{\partial^2 w}{\partial z^2} - \left(\frac{z}{H^2}\right)\frac{\partial w}{\partial z} + \left[\left(\frac{\hat{\omega}^2 - \Omega_\perp^2}{\Omega_\perp^2}\right)\frac{1}{H^2} - \left(\frac{\hat{\omega}^2}{\hat{\omega}^2 - \kappa^2}\right)k^2\right]w = 0. \tag{31}$$

This equation can be transformed into the parabolic cylinder equation (Abramowitz & Stegun 1965, hereafter AS). We will be concerned with solutions for which both k and $\hat{\omega}$ are real.

4.2.1. *Transformation of the equation*

The substitution

$$w(z) = y(x)\exp\left(\tfrac{1}{4}x^2\right), \tag{32}$$

where

$$x = \frac{z}{H}, \tag{33}$$

transforms equation (31) into

$$\frac{d^2y}{dx^2} - \left(\tfrac{1}{4}x^2 + a\right)y = 0, \tag{34}$$

where

$$a = \left(\frac{\hat{\omega}^2}{\hat{\omega}^2 - \kappa^2}\right) k^2 H^2 - \left(\frac{\hat{\omega}^2 - \Omega_\perp^2}{\Omega_\perp^2}\right) - \tfrac{1}{2}. \quad (35)$$

Two linearly independent solutions are $U(a,x)$ and $V(a,x)$, defined by AS. The asymptotic forms as $x \to +\infty$ are (AS, eq. [19.8])

$$U(a,x) \sim x^{-(a+1/2)} \exp\left(-\tfrac{1}{4}x^2\right), \quad (36)$$

$$V(a,x) \sim \left(\frac{2}{\pi}\right)^{1/2} x^{a-1/2} \exp\left(\tfrac{1}{4}x^2\right). \quad (37)$$

4.2.2. *Conditions at $z = \pm\infty$*

In order to select physically acceptable solutions, we must examine the behavior of the wave action as $|z| \to \infty$. A suitable energy wave action can be defined, whose density, averaged over time, is

$$\mathcal{A}^{(e)} = \frac{\rho\omega}{2\hat{\omega}} \left(|u|^2 + |w|^2\right), \quad (38)$$

and whose vertical flux, also averaged over time, is

$$\mathcal{F}_z^{(e)} = \mathrm{Re}\left(w^* p'\right). \quad (39)$$

In the case of the isothermal layer, the limiting behavior of the wave action as $z \to +\infty$ is

$$\mathcal{A}^{(e)} \propto x^{1-2a} \exp\left(-\tfrac{1}{2}x^2\right), \quad (40)$$

$$\mathcal{F}_z^{(e)} \propto x^{-2a} \exp\left(-\tfrac{1}{2}x^2\right) \quad (41)$$

for the solution $U(a,x)$, and

$$\mathcal{A}^{(e)} \propto x^{1+2a} \exp\left(\tfrac{1}{2}x^2\right), \quad (42)$$

$$\mathcal{F}_z^{(e)} \propto x^{2a} \exp\left(\tfrac{1}{2}x^2\right) \quad (43)$$

for the solution $V(a,x)$. It is clear that only the solution $U(a,x)$ is acceptable at $z = +\infty$. Similarly, only the solution $U(a,-x)$ is acceptable at $z = -\infty$. These solutions represent evanescent waves at infinity.

4.2.3. *Modes in a purely isothermal disk*

When the disk is purely isothermal without a polytropic layer, we recover the results of LP as follows. An acceptable solution for $y(x)$ must be proportional to both $U(a,x)$ and $U(a,-x)$. However, these functions are linearly dependent only when $a = -n - \frac{1}{2}$, with n a nonnegative integer. In that case

$$U(-n-\tfrac{1}{2},x) = 2^{-n/2} H_n\left(2^{-1/2}x\right) \exp\left(-\tfrac{1}{4}x^2\right), \quad (44)$$

where H_n is the Hermite polynomial of degree n (AS, eq. [19.13.1]). This condition leads to the dispersion relation

$$n = \left(\frac{\hat{\omega}^2 - \Omega_\perp^2}{\Omega_\perp^2}\right) - \left(\frac{\hat{\omega}^2}{\hat{\omega}^2 - \kappa^2}\right) k^2 H^2 \quad (45)$$

equivalent to equation (54) of LP for the case $\gamma = 1$.

4.3. *Numerical solutions in the polytropic layer*

The equations in the polytropic layer must be solved numerically, as in Korycansky & Pringle (1995). In a form similar to equations (28) and (29), they are

$$\frac{\partial u}{\partial z} = \left[s - \left(\frac{s+1}{\gamma}\right)\right] \left(\frac{2z}{H_s^2 - z^2}\right) u + \left(\frac{ik}{\hat{\omega}^2 - \kappa^2}\right) \times \left\{\hat{\omega}^2 - \Omega_\perp^2 \left[s - \left(\frac{s+1}{\gamma}\right)\right] \left(\frac{2z^2}{H_s^2 - z^2}\right)\right\} w \quad (46)$$

and

$$\frac{\partial w}{\partial z} = \left(\frac{1}{ik}\right) \left[k^2 - \left(\frac{s+1}{\gamma}\right) \left(\frac{\hat{\omega}^2 - \kappa^2}{\Omega_\perp^2}\right) \left(\frac{2}{H_s^2 - z^2}\right)\right] u + \left(\frac{s+1}{\gamma}\right) \left(\frac{2z}{H_s^2 - z^2}\right) w. \quad (47)$$

The boundary conditions at $z = 0$ are the usual symmetry conditions,

$$\frac{\partial u}{\partial z} = w = 0 \quad (48)$$

for an even mode, and

$$u = \frac{\partial w}{\partial z} = 0 \quad (49)$$

for an odd mode. At $z = z_1$, the solutions must be matched on to the solutions in the isothermal layer. Both u and w must be continuous.

The matching condition is

$$\frac{u}{w} = ikH \left[k^2 H^2 - \left(\frac{\hat{\omega}^2 - \kappa^2}{\Omega_\perp^2}\right)\right]^{-1} \left[\frac{U'(a,x_1)}{U(a,x_1)} - \frac{x_1}{2}\right]. \quad (50)$$

where $x_1 = z_1/H$, and the prime denotes differentiation with respect to the (second) argument. (If this ratio diverges, the matching condition is $w = 0$.)

The numerical method is as follows. A value of k and a symmetry (either even or odd) are chosen. The values of u and w at $z = 0$ are determined by the appropriate symmetry condition and by an arbitrary normalization condition. The value of $\hat{\omega}$ must be guessed. The equations are then integrated from $z = 0$ to $z = z_1$, and the value of $\hat{\omega}$ tuned so that the matching condition is satisfied.

To evaluate the function $U(a,x)$ and its derivative numerically, we use the following method. When $a > 0$ and $x^2 + 4a \gg 1$, Darwin's expansion (AS, eq. [19.10.2]) provides an accurate asymptotic approximation. If these conditions are not satisfied, we choose a positive integer N such that $U(a+N,x)$ and $U(a+N+1,x)$ can be evaluated accurately using Darwin's expansion. These values are used to initialize the recurrence relation

$$U(a+n-1,x) = xU(a+n,x) + (a+n+\tfrac{1}{2})U(a+n+1,x) \quad (51)$$

(AS, eq. [19.6.4]), which is then iterated to determine $U(a,x)$. (The recurrence is stable in this direction.) Finally, the recurrence relation

$$U'(a,x) = -\tfrac{1}{2}xU(a,x) - (a+\tfrac{1}{2})U(a+1,x) \quad (52)$$

(AS, eq. [19.6.1]) provides the derivative.

4.4. *Asymptotic solutions in the limit $kH \to \infty$*

As waves propagate radially away from the resonances where they are excited, the dispersion relation is often followed into a limit in which kH is large. This can lead to wave channeling, as described in Paper I, and it is important to determine the behavior of the modes in this limit so that the effects of nonlinear dissipation can be estimated.

In a purely polytropic disk, Ogilvie (1998) showed that the f, p, and g modes all become trapped near the surfaces of the disk in this limit, and have $\hat{\omega}^2/\Omega_\perp^2 = O(kH)$. In contrast, the r modes become trapped near the mid-plane, and have $\hat{\omega}^2/\Omega_\perp^2 = O\left((kH)^{-1}\right)$. (In the exceptional case when the disk is marginally stable to convection, the r modes have $\hat{\omega}^2/\Omega_\perp^2 = O\left((kH)^{-2}\right)$ and do not become localized.)

In a purely isothermal disk, the limiting behavior of the dispersion relation (45) is easily found to be

$$\hat{\omega}^2 = c^2k^2 + \kappa^2 + (n+1)\Omega_\perp^2 + O\left((kH)^{-2}\right) \tag{53}$$

for the p modes, and

$$\hat{\omega}^2 = (n+1)\frac{\kappa^2}{k^2H^2} + O\left((kH)^{-4}\right) \tag{54}$$

for the r modes. Evidently the 2D mode may be considered to correspond to the case $n = -1$ in equation (53).

For the mixed model considered in this paper, it is clear that the limiting behavior of the r modes will agree with the purely polytropic case and will not be affected by the outer layers (except in the marginally stable case). This cannot be true of the other modes, however, since the surface at which they would have become concentrated is no longer present. Instead, the wave action moves out into the isothermal layer. We seek a solution in which, in accordance with the behavior of all modes other than r modes in the purely isothermal disk,

$$\hat{\omega}^2 = c^2k^2 + \kappa^2 + (\tfrac{1}{2} - \hat{a})\Omega_\perp^2 + O\left((kH)^{-2/3}\right), \tag{55}$$

where $\hat{a}$ is a constant to be determined. (The scaling of the remainder term will be seen later to be justified.) Then

$$a = \hat{a} + O\left((kH)^{-2/3}\right). \tag{56}$$

The matching condition at $z = z_1$ is, from equation (50),

$$\frac{u}{w} = -\frac{ikH}{(\frac{1}{2} - \hat{a})}\left[\frac{U'(\hat{a}, x_1)}{U(\hat{a}, x_1)} - \frac{x_1}{2}\right] + O\left((kH)^{1/3}\right). \tag{57}$$

Now consider the limiting form of the equations in the polytropic layer. A first examination of equations (46) and (47) yields

$$\frac{\partial u}{\partial z} \sim ikw \tag{58}$$

and

$$\frac{\partial w}{\partial z} \sim -ik\left(\frac{z_1^2 - z^2}{H_s^2 - z^2}\right)u, \tag{59}$$

which imply

$$\frac{\partial^2 u}{\partial z^2} \sim k^2\left(\frac{z_1^2 - z^2}{H_s^2 - z^2}\right)u. \tag{60}$$

The solution in $z < z_1$ is an evanescent WKB function, but there is a turning point at $z = z_1$. In the neighborhood of the interface, the solution must be described using an Airy function. For $(z_1 - z)/z_1 = O\left((kH)^{-2/3}\right)$, one finds

$$u \sim Ai\left[\left(\frac{2z_1}{H_s^2 - z_1^2}\right)^{1/3} k^{2/3}(z_1 - z)\right], \tag{61}$$

$$w \sim ik^{-1/3}\left(\frac{2z_1}{H_s^2 - z_1^2}\right)^{1/3} \times Ai'\left[\left(\frac{2z_1}{H_s^2 - z_1^2}\right)^{1/3} k^{2/3}(z_1 - z)\right], \tag{62}$$

subject to an arbitrary normalization, and so

$$\frac{u}{w} \sim -ik^{1/3}\left(\frac{2z_1}{H_s^2 - z_1^2}\right)^{-1/3}\left[\frac{Ai(0)}{Ai'(0)}\right] = O\left((kH)^{1/3}\right) \tag{63}$$

at the interface. For consistency with equation (57), we require

$$\frac{U'(\hat{a}, x_1)}{U(\hat{a}, x_1)} - \frac{x_1}{2} = 0. \tag{64}$$

This transcendental equation for $\hat{a}$ has infinitely many roots, each of which corresponds to the limiting form of one branch of the dispersion relation, according to equation (55).

5. PROPAGATION OF THE F MODE

5.1. *Numerical results*

As in Paper I, we focus of the properties of the f^e mode, since it is by far the dominant mode excited at an LR. In obtaining numerical solutions, we have considered a Keplerian disk whose polytropic layer has index $s = 3$ and adiabatic exponent $\gamma = 5/3$. We have examined four different values of the effective optical depth: $\tau = 10$, 100, 1000 and 10000. The parameters of the four models are summarized in Table 1. The quantities given are the ratio Σ_i/Σ_p of the surface densities of the isothermal and polytropic layers, the ratio T_i/T_m of the temperature of the isothermal atmosphere to the temperature at the midplane, the dimensionless height z_1/H_s of the interface, the dimensionless scale height H/H_s of the atmosphere, the fraction f of the torque exerted at an LR that is carried by the f^e mode, and the eigenvalue $\hat{a}$ of equation (64) corresponding to the f^e mode.

In Figure 1 we plot the dispersion relation for the f^e mode in the four models. This is compared with the dispersion relation for a purely polytropic disk and also with the limiting form given by equation (55). It can be seen that the purely polytropic dispersion relation provides a good approximation until the wave action of the mode migrates into the atmosphere, at which point the approximation given by equation (55) becomes good. The value of kH_s at which this transition occurs increases with increasing τ. Note that the eigenvalue $\hat{a}$ is a negative number whose magnitude increases with increasing τ. According to the correspondence $\hat{a} = -n - \frac{1}{2}$, this means that, in an optically thick disk, the atmospheric part of the eigenfunction of the f^e mode does not resemble the 2D mode

TABLE 1
PARAMETERS OF THE FOUR MODELS.

τ	Σ_i/Σ_p	T_i/T_m	z_1/H_s	H/H_s	f	$\hat{a}$
10	1.266×10^{-1}	0.7186	0.5305	0.2997	0.9771	−2.558
100	8.872×10^{-3}	0.4041	0.7719	0.2248	0.9687	−5.751
1000	8.025×10^{-4}	0.2272	0.8791	0.1685	0.9679	−10.587
10000	7.670×10^{-5}	0.1278	0.9339	0.1264	0.9678	−18.529

of a purely isothermal disk, but is more like the tail of a high-order p mode after its final node.

We now consider the propagation of the f^e mode away from an LR, as in Paper I. Away from the resonance, the radial flux of angular momentum associated with the wave (averaged over t, integrated over ϕ and z),

$$F^{(a)} = \frac{\pi r m}{k}\left(\frac{\hat{\omega}^2 - \kappa^2}{\hat{\omega}^2}\right)\int \rho |u|^2 \, dz, \tag{65}$$

is independent of r, and this condition determines the relative normalization of the wave at each radius. Our method of estimating the nonlinearity of the wave at each radius is to locate the value of z at which the peak of the density of angular momentum wave action (averaged over t),

$$\mathcal{A}^{(a)} = \left(\frac{m}{2\hat{\omega}}\right)\rho\left(|u|^2 + |w|^2\right), \tag{66}$$

occurs, and to compute the (isothermal) Mach number of the RMS velocity perturbation,

$$\mathcal{M} = \left[\frac{\frac{1}{2}\left(|u|^2 + |v|^2 + |w|^2\right)}{p/\rho}\right]^{1/2}, \tag{67}$$

at that height.

Since this measure depends on the overall amplitude of the wave, we normalize it in terms of its value at the resonance as follows. In the neighborhood of the LR, the horizontal components of the velocity dominate, and the peak of the wave action density occurs on $z = 0$. The form of the inner solution is (cf. Paper I)

$$u \sim C\tilde{u}(z)\left[Ai(qx) \pm iGi(qx)\right], \tag{68}$$
$$v \sim iC\tilde{v}(z)\left[Ai(qx) \pm iGi(qx)\right], \tag{69}$$

where $x = (r - r_L)/r_L$, C is a constant, q and $\tilde{u}(z)$ are the f-mode eigenvalue and eigenfunction discussed in Paper I, and $\tilde{v} = -(2B/\hat{\omega})\tilde{u}$. The constant C is determined by asymptotic matching to the WKB solution away from the LR. Now the maximum value of $[Ai(qx)]^2 + [Gi(qx)]^2$ is approximately 0.3603 and occurs at $qx \approx -1.845$. This determines the maximum Mach number at the LR, which we call $\mathcal{M}_L$. The scalings are such that $\mathcal{M}/\mathcal{M}_L$ away from resonance is $O\left((H_s/r)^{1/6}\right)$, and for this reason we evaluate the quantity

$$\left(\frac{\mathcal{M}}{\mathcal{M}_L}\right)\left(\frac{r}{H_s}\right)^{1/6}. \tag{70}$$

As in Paper I, we have assumed that the disk is Keplerian, so that the dimensionless intrinsic frequency of the wave is given by

$$\frac{\hat{\omega}}{\Omega} = m\left[\left(\frac{r}{r_c}\right)^{3/2} - 1\right], \tag{71}$$

where r_c is the corotation radius of the mode. We have also assumed that $H_s \propto H \propto r$ and $\Sigma \propto r^{-1}$. This variation of parameters was selected so that the wave Mach number would be finite at the radial center of the disk. In this way, we have removed geometrical focusing effects from the wave-channeling effects of interest in this paper.

In Figure 2 we plot the variation with r of the height z_{peak} of the local vertical peak in the wave action density. We consider both inward propagation from the inner LR and outward propagation from the outer LR; we consider azimuthal wave numbers $m = 2$ and $m = 10$; and we consider the four models with different optical depths. In Figure 3 we plot the quantity in equation (70) for each of these cases. As Figure 2 shows, the f mode is launched at resonance with the peak of wave action density located at the mid-plane and the peak rises away from the mid-plane as it propagates away from the resonance. When z_{peak} reaches the base of the atmosphere, it resides there over a non-zero interval in radius, as is apparent in Figure 2 by the flat slope of the curves. This discontinuous behavior of the slope is caused by our idealization of the transition from the polytropic interior to the isothermal atmosphere as occurring abruptly in the vertical direction. Notice that the rise of z_{peak} with distance from the resonance increases with optical depth. However, the peak never rises to great heights in the atmosphere. Figure 4 shows how the wave action density is distributed vertically.

We have verified that the waves are not artificially confined within the disk in our model, either by the discontinuity in the sound speed at the interface (which results from a change in the effective adiabatic exponent) or by the discontinuity in the buoyancy frequency. If the isothermal layer is treated as having an adiabatic exponent equal to that of the polytropic layer, so that the sound speed is everywhere continuous, the wave migrates into the atmosphere at nearly the same stage during the radial propagation. The peak of the wave action density rises only slightly higher than in the case of a truly isothermal atmosphere. If, instead, the disk is treated as adiabatically stratified in both layers, so that the buoyancy frequency is everywhere continuous (and zero), the results are almost

indistinguishable from those we have presented here. We emphasize that radially propagating waves in an accretion disk are generically confined in the vertical direction because the vertical gravity increases with height above the mid-plane.

6. SUMMARY AND DISCUSSION

We have analyzed the effects of a disk atmosphere on the propagation of a wave, the f mode, launched from a Lindblad resonance in a thermally stratified disk. The atmosphere was modeled as an isothermal layer that resides above a polytropic region that extends down to the mid-plane. The polytropic region represents the (vertically) optically thick interior of the disk. The effects of the atmosphere can be important because the f mode becomes progressively more confined to the disk surface with distance from resonance. The wave energy is concentrated in the vertical direction as the wave propagates radially (see Figure 4). The peak of wave action density in the disk follows the trajectories shown in Figure 2 for various values of azimuthal wavenumber m and disk optical depth τ. The dominant amplification of a wave occurs in the thermally stratified region below the disk atmosphere through the process of wave channeling, as was anticipated in Paper I (see the discussion in §8.2). The disk atmosphere lessens the degree of wave amplification.

As was found in Paper I, the launched wave (f mode) behaves more like a surface gravity wave as it propagates radially away from the resonance. In a purely vertically polytropic disk with no atmosphere, the vertical extent of the surface gravity wave decreases with increasing radial distance from resonance. As a result, there is usually a substantial increase in wave amplitude on a radial scale of order $r_{\rm L}/m$ from resonance, through a process termed wave channeling. In the presence of an atmosphere, the effects of wave channeling are lessened (see Figure 3). The increase in wave amplitude becomes limited once the wave enters the disk atmosphere. For disks of smaller optical depths, the thermal stratification is small and the wave enters the isothermal layer on a radial scale somewhat smaller than $r_{\rm L}/m$. Consequently, the wave behaves more like the 2D acoustic mode at most radii, in accordance with the expected limiting behavior of a vertically isothermal disk, in which the wave is 2D at all radii and its peak never rises above the mid-plane.

For disks around individual stars (circumstellar disks) in close binary star systems ($m = 2$), the increase in wave Mach number from resonance to disk center is typically less than a factor of 10, and somewhat less for lower optical depths (see Figure 3a). For disks around binary star systems (circumbinary disks) ($m = 2$) the increase in wave Mach number from resonance is large over a scale of order the resonance radius (see Figure 3c). For waves that are mildly nonlinear at resonance, nonlinear wave damping is likely to be important in such disks of modest vertical optical depth ($\tau > 10$). These effects are much stronger for circumbinary, rather than circumstellar disks.

For protostellar disks ($m \sim 10$, see Figure 3b and 4b), planet-forming regions are expected to be optically thick (Bell et al. 1997). Typical wave velocities near a giant planet are likely to be mildly supersonic, with Mach number around 0.2 (Goldreich & Tremaine 1979). In such a situation, wave channeling would likely lead to shocks for disks of moderate optical depths (of order 100) on a radial scale of a few times the disk thickness.

We emphasize that the detailed nonlinear outcome of the wave-channeling process remains uncertain. While the wave action is concentrated in the polytropic layer, the motion is approximately incompressible, but this is no longer true once the wave migrates into the atmosphere, where shocks may limit the amplitude. For this reason we have used the Mach number of the wave motion as a measure of nonlinearity. The development of shocks or other nonlinear wave phenomena under these circumstances could be usefully investigated using numerical simulations.

We gratefully acknowledge support from NASA Origins of Solar Systems Grants NAGW-4156 and NAG5-4310, and NATO travel grant CRG940189. We acknowledge the support and hospitality of the Isaac Newton Institute for Mathematical Sciences. We thank Jim Pringle for many discussions on this problem.

REFERENCES

Abramowitz, M., & Stegun, I. A. 1965, Handbook of Mathematical Functions (New York: Dover) (AS)
Bell, K. R., Cassen, P. M., Klahr, H. H., & Henning, Th. 1997, ApJ, 486, 372
Cassen, P., & Woolum, D. S. 1996, ApJ, 472, 789
Goldreich, P., & Tremaine, S. 1979, ApJ, 233, 857
Korycansky, D. G., & Pringle, J. E. 1995, MNRAS, 272, 618
La Dous, C. 1994, Space Science Reviews, 67, 1
Lubow, S. H., & Ogilvie, G. I. 1998, ApJ, in press (Paper I)
Lubow, S. H., & Pringle, J. E. 1993, ApJ, 409, 360 (LP)
Ogilvie, G. I. 1998, MNRAS, in press

FIG. 1.— Local dispersion relation (*solid line*) for the f^e mode in a Keplerian disk consisting of a polytropic layer with $s = 3$ and $\gamma = 5/3$ matched to an isothermal atmosphere. The four panels correspond to optical depths $\tau = 10$, 100, 1000, and 10000. *Dotted line*: dispersion relation for a purely polytropic disk ($\tau = \infty$). *Dashed line*: asymptotic approximation given in equation (55).

FIG. 2.— Height of the peak of the wave action density as the f^e mode propagates away from an LR. *Solid line*: $\tau = 10$. *Dotted line*: $\tau = 100$. *Dashed line*: $\tau = 1000$. *Dot-dashed line*: $\tau = 10000$. *Panel (a)*: inner LR, $m = 2$. *Panel (b)*: inner LR, $m = 10$. *Panel (c)*: outer LR, $m = 2$. *Panel (d)*: outer LR, $m = 10$.

FIG. 3.— RMS Mach number of the velocity perturbation at the peak of the wave action density, relative to its value at the resonance. The vertical scale is logarithmic. *Panel (a)*: inner LR, $m = 2$. *Solid line*: $\tau = 10$. *Dotted line*: $\tau = 100$. *Dashed line*: $\tau = 1000$. *Dot-dashed line*: $\tau = 10000$. *Panel (b)*: inner LR, $m = 10$. *Panel (c)*: outer LR, $m = 2$. *Panel (d)*: outer LR, $m = 10$.

FIG. 4.— Eigenfunctions of the f^e mode. The wave action density is plotted as a function of the vertical coordinate for two different values of the radial wavenumber. The modes are normalized so that the wave action density integrates to unity over the full vertical extent of the disk. *Panel (a)*: $kH_s = 10$. *Solid line*: $\tau = 10$. *Dotted line*: $\tau = 100$. *Dashed line*: $\tau = 1000$. *Dot-dashed line*: $\tau = 10000$. *Panel (b)*: $kH_s = 100$.

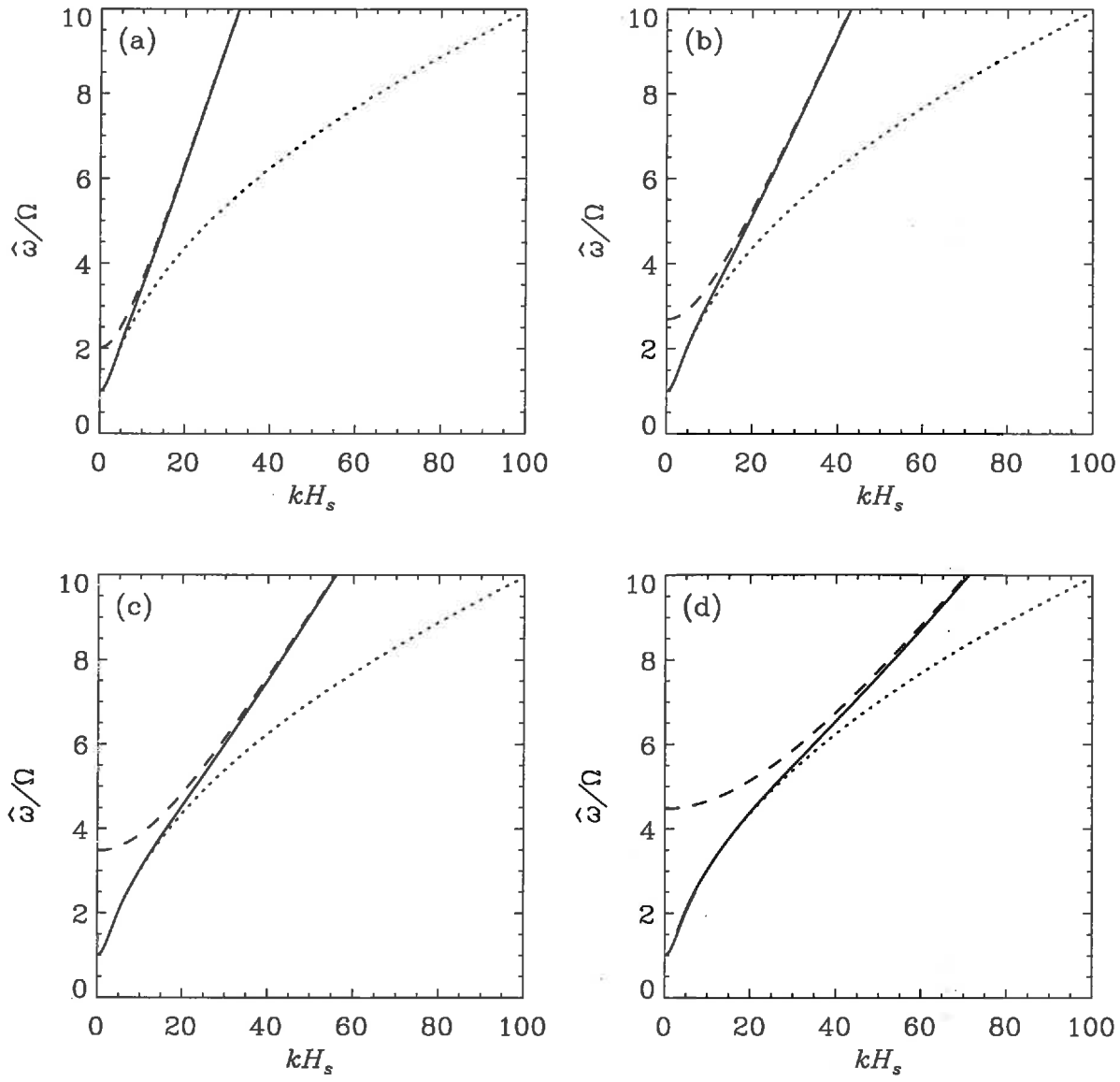

Figure 1

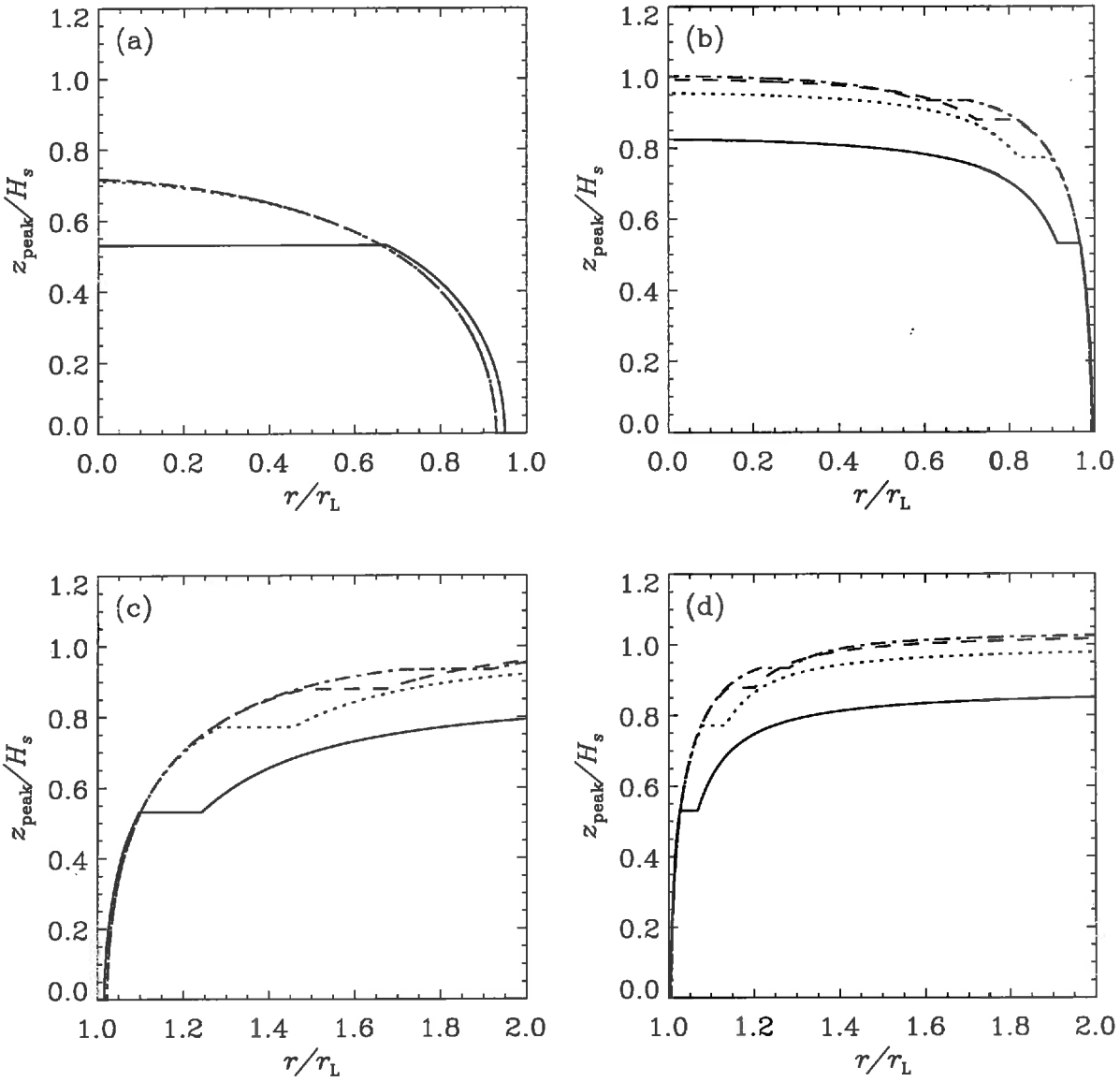

Figure 2

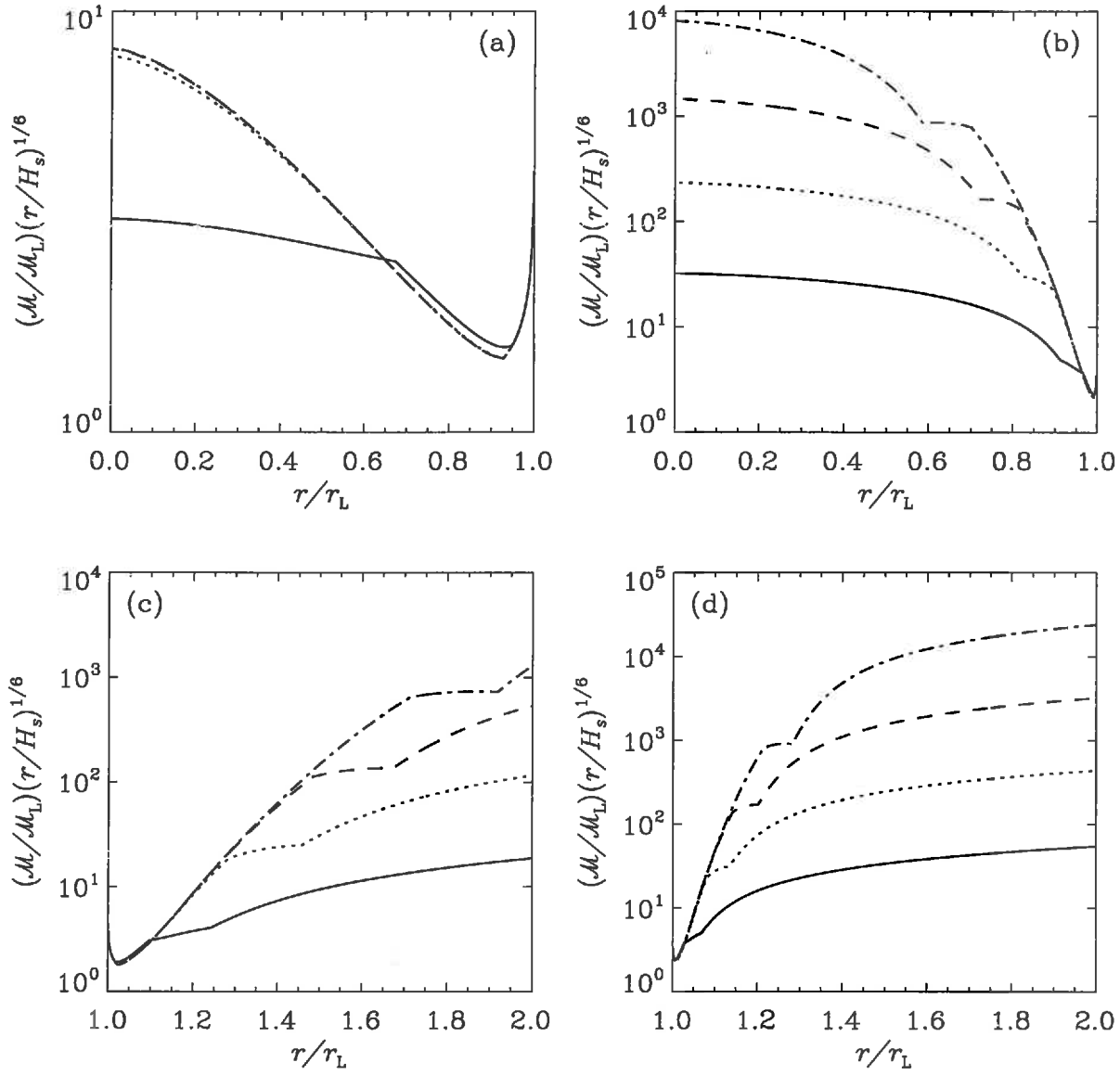

Figure 3

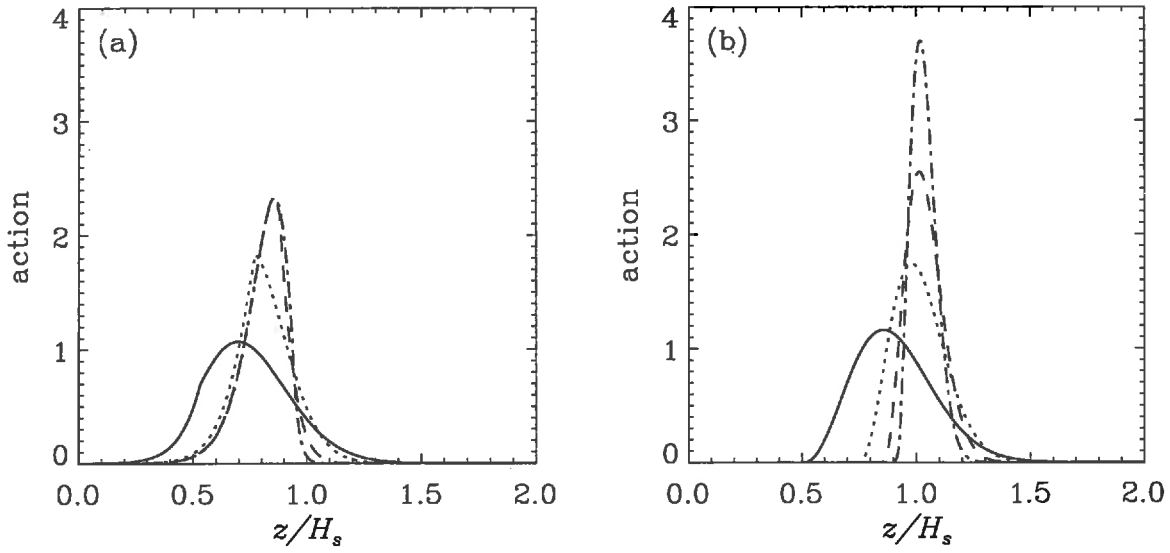

Figure 4

Recent Newton Institute Preprints

NI97019-NQF **N Dorey, VV Khoze and MP Mattis**
Instantons, three-dimensional gauge theory and the Atiyah-Hitchin manifold
hep-th/9703228; Phys.Lett. B408 (1997) 213-221

NI97020-NQF **N Dorey, VV Khoze, MP Mattis et al**
Multi-instantons, three-dimensional guage theory, and the Gauss-Bonnet-Chern theorem
hep-th/9704197; Nucl.Phys. B502 (1997) 94-106

NI97021-NQF **JM Figueroa-O'Farrill, C Köhl and B Spence**
Supersymmmetry and the cohomology of (hyper) Kähler manifolds
hep-th/9705161; Nucl.Phys. B503 (1997) 614-626

NI97022-NQF **JP Gauntlett**
Duality and supersymmetric monopoles
hep-th/9705025; Nucl.Phys.Proc.Suppl. 61A (1998) 137-148

NI97023-NQF **JP Gauntlett**
Intersecting branes
hep-th/9705011

NI97024-RAG **J Rickard**
Triangulated categories in the modular representation theory of finite groups

NI97025-NQF **P van Baal**
Intermediate volumes and the role of instantons

NI97026-NQF **CJ Houghton, NS Manton and PM Sutcliffe**
Rational maps, monopoles and skyrmions
hep-th/9705151; Nuclear Physics B510 [PM] (1998) 507-537

NI97027-NQF **PS Howe, E Sezgin and PC West**
Aspects of superembeddings
hep-th/9705903

NI97028-NQF **CM Hull**
Gravitational duality, branes and charges
hep-th/9705162; Nucl.Phys. B509 (1998) 216-251

NI97029-NQF **M Abou Zeid and CM Hull**
Instrinsic geometry of D-branes
hep-th/9704021; Phys.Lett. B404 (1997) 264-270

NI97030-NQF **CP Bachas, MR Douglas and MB Green**
Anomalous creation of branes
hep-th/9705074

NI97031-RAG **M Broué, G Malle and J Michel**
Complex reflection groups, braid groups, Hecke algebras

NI97032-NQF **D Zwanziger**
Renormalization in the Coulomb gauge and order parameter for confinement in QCD

NI97033-NQF **E Shuryak and A Zhitnisky**
The gluon/charm content of the $\eta\prime$ meson and instantons
hep-ph/9706316; Phys.Rev. D57 (1998) 2001-2004

NI97035-RAG **K Magaard and G Malle**
Irreducibility of alternating and symmetric squares

NI97036-STA **N Linden and S Popescu**
On multi-particle entanglement

NI97037-NNM **M Studeny and RR Bouckaert**
On chain graph models for description of conditional independence structures

NI97038-RAG **M Geck and G Malle**
On special pieces in the unipotent variety

NI97039-NNM **SP Luttrell**
A unified theory of density models and auto-encoders
DERA report DERA/CIS/CIS5/651/FUN/STIT/5-4 31 October 1997

NI97040-NNM **CKI Williams and D Barber**
Bayesian Classification with Gaussian Processes

NI97041-NNM **TS Richardson**
Chain graphs and symmetric associations

NI97042-NNM **A Roverato and J Whittaker**
An importance sampler for graphical Gaussian model inference

NI97043-DQC **MR Haggerty, JB Delos, N Spellmeyer et al**
Extracting classical trajectories from atomic spectra

NI97044-DQC **S Zelditch**
Large level spacings for quantum maps in genus zero

NI97045-DQC **U Smilansky**
Semiclassical quantization of maps and spectral correlations

NI97046-DQC **IY Goldscheid and BA Khoruzhenko**
Distribution of Eigenvalues in non-Hermitian Anderson models
Phys. Rev. Lett. 80 (1998) No.13, 2897-2900

NI97047-DQC **G Casati, G Maspero and DL Shepelyansky**
Quantum fractal Eigenstates

NI98001-STA **N Linden and S Popescu**
Non-local properties of multi-particle density matrices

NI98002-AMG **J-L Colliot-Thélène**
Un principe local-global pour les zéro-cycles sur les surfaces fibrés en coniques au-dessus d'une courbe de genre quelconque

NI98003-AMG **RGE Pinch and HPF Swinnerton-Dyer**
Arithmetic of diagonal quartic surfaces, II

NI98004-AMG **DR Heath-Brown**
The solubility of diagonal cubic diophantine equations

NI98005-AMG **B Poonen and M Stoll**
The Cassels-Tate pairing on polarized Abelian varieties

NI98006-AMG **P Parimala and V Suresh**
Isotropy of quadratic forms over function fields of curves over p-adic fields

NI98007-AMG **E Peyre**
Application of motivic complexes to negligible classes

NI98008-AMG **E Peyre**
Torseurs universels et méthode du cercle

NI98009-RAG **JA Green**
Discrete series characters for $GL(n, q)$

NI98010-DQC **K Zyczkowski**
On the volume of the set of mixed entangled states

NI98011-DQC **K Zyczkowski**
Monge distance between quantum states

NI98012-DAD **JA Sellwood, RW Nelson and S Tremaine**
Resonant thickening of disks by small satellite galaxies

NI98013-DAD **GI Ogilvie and SH Lubow**
The effect of an isothermal atmosphere on the propagation of three-dimensional waves in a thermally stratified accretion disk

---